SANDIA REPORT
SAND2006-6063
Unlimited Release
Printed March 2007

Development of the Doppler Electron Velocimeter—Theory

Phillip L. Reu

Prepared by
Sandia National Laboratories
Albuquerque, New Mexico 87185 and Livermore, California 94550

Sandia is a multiprogram laboratory operated by Sandia Corporation,
a Lockheed Martin Company, for the United States Department of Energy's
National Nuclear Security Administration under Contract DE-AC04-94AL85000.

Approved for public release; further dissemination unlimited.

Issued by Sandia National Laboratories, operated for the United States Department of Energy by Sandia Corporation.

Available to DOE and DOE contractors from
U.S. Department of Energy
Office of Scientific and Technical Information
P.O. Box 62
Oak Ridge, TN 37831

Telephone: (865) 576-8401
Facsimile: (865) 576-5728
E-Mail: reports@adonis.osti.gov
Online ordering: http://www.osti.gov/bridge

Available to the public from
U.S. Department of Commerce
National Technical Information Service
5285 Port Royal Rd.
Springfield, VA 22161

Telephone: (800) 553-6847
Facsimile: (703) 605-6900
E-Mail: orders@ntis.fedworld.gov
Online order: http://www.ntis.gov/help/ordermethods.asp?loc=7-4-0#online

SAND2006-6063
Unlimited Release
Printed March 2007

Development of the Doppler Electron Velocimeter—Theory

Phillip L. Reu
Applied Mechanics Development
Sandia National Laboratories
P.O. Box 5800
Albuquerque, New Mexico 87185-1070

Abstract

Measurement of dynamic events at the nano-scale is currently impossible. This paper presents the theoretical underpinnings of a method for making these measurements using electron microscopes. Building on the work of Möllenstedt and Lichte who demonstrated Doppler shifting of an electron beam with a moving electron mirror, further work is proposed to perfect and utilize this concept in dynamic measurements. Specifically, using the concept of "fringe-counting" with the current principles of transmission electron holography, an extension of these methods to dynamic measurements is proposed. A presentation of the theory of Doppler electron wave shifting is given, starting from the development of the de Broglie wave, up through the equations describing interference effects and Doppler shifting in electron waves. A mathematical demonstration that Doppler shifting is identical to the conceptually easier to understand idea of counting moving fringes is given by analogy to optical interferometry. Finally, potential developmental experiments and uses of a Doppler electron microscope are discussed.

ACKNOWLEDGMENTS

The author thanks Paul Kotula, Bruce Hansche, and Jack Houston for critically reviewing this document and their valuable input as the idea has developed. Special appreciation is given to Edgar Voelkl for his valuable input and experience in this area.

CONTENTS

FIGURES

TABLES

This page intentionally left blank.

NOMENCLATURE

DEV	Doppler electron velocimeter
FEG	field emission gun
LDV	laser Doppler velocimeter
MEMS	microelectromechanical systems
SEM	scanning electron microscope
TEM	transmission electron microscope

p	momentum
m	mass
v	velocity
c	velocity of light
F	force
t	time
W	work
K	kinetic energy
m_o	rest mass
E	energy
ΔE	energy spread
h	Plank's constant
$\hbar$	$h/2\pi$
e	electron charge
E	electric field
B	magnetic field
U	accelerating potential
$\vec{k}$	wave number
λ	wave length
Ψ	wavefunction
ϕ	phase
I	irradiance or intensity
$\Delta\tau$	emission time
Δz	longitudinal coherence
Δx	transverse coherence or displacement
ω	angular velocity
j	beam current
β	source brightness

This page intentionally left blank.

1. INTRODUCTION

The Doppler electron velocimeter (DEV) is a new measurement concept motivated by the increasing importance of nano-scale engineering. As background, microelectromechanical systems (MEMS) have benefited greatly from examination of the dynamical characteristics of the system. These measurements have traditionally been done using laser Doppler velocimeters (LDVs) to scan the part while it is undergoing excitation to examine the resulting modal shapes. These investigations have yielded significant information critical to the design, fabrication, and use of MEMS products. The limitation of LDVs is their use of visible wavelengths for the probe laser beams. As components continue to shrink, the diffraction limitations of the optical microscopes used will disallow the use of this technique. This is true even now for some specialized MEMS devices that use line widths that are less than one-half micron in size or in biological investigations where the cells or cellular features are too small to be probed by the laser. This problem will continue to worsen as researchers push from the micro to the nano regimes. Current nano-scale research is typically in the materials research area. Even this field could benefit from a technique to measure dynamical events at the sub-micron scale. The DEV is being developed to meet these needs. This paper covers the theoretical underpinnings for the development of the DEV starting with a transmission electron microscope (TEM) as a platform for development. The electron microscope community has invested millions of dollars in developing optics, electron sources, and detectors that can be used to make dynamic measurements at the nano-scale: that is at least the contention of this theory paper.

1.1. Introduction to Doppler Electrons

The wave-particle duality concept leads to many interesting phenomena, including the concept that particles can destructively and constructively interfere. This connection was first made by Louis de Broglie, in his doctoral thesis (1924), where he proposed the concept that if light might be particles (photons), maybe particles are waves. Subsequent experimentation conducted using electron diffraction from crystals (Davisson, Germer, and Thompson) conclusively demonstrated this. These experiments have since been extended to both neutrons and atoms [1,2]. Gabor, while working with early electron microscopes, proposed using holography to cancel out the effects of spherical aberrations in early microscope images [3]. He went on to create optical holography using coherent light and photographic techniques to capture the complete information of the light wavefront.

The electron microscope, which inspired Gabor, has progressed significantly since the 1950s. Commercial transmission electron microscope systems are available with coherent sources of good brightness and are even optimized specifically for holography (Hitachi HF-2000). At this point, electron analogs for nearly all the traditional optical components required for holography have been demonstrated, including beam-splitters, mirrors, and prisms. Following in the tradition of the classical interferometric experiments of Fizeau, Michelson, Rayleigh, and Fabry and Perot in the optical domain, researchers have conducted similar experiments using the new technology of electron microscopes [4,5], including the traditional interferometric arrangements of Young's double hole [6], the Fresnel biprism [7], and Mach-Zehnder [8] and Michelson [9] interferometers. A number of good review papers and books cover in more detail the general concepts of electron holography, including Tonomura [10], Missiroli [11], and Völkl [12].

This paper concerns Doppler interferometry, often referred to as velocimetry. In the literature search, only two papers have been published on Doppler effects with electron microscopes. Möllenstedt and Lichte have demonstrated the effect of using a rotating electron mirror in a Michelson interferometer [13], with good results. Although the paper is only two pages, it shows the Doppler modulation of two beams reflected at different velocities and recombined. The other is a companion paper on the theoretical treatment of this topic by Scherzer [14]. Since the late 1970s, the concept of Doppler velocimetry with electrons has not been investigated to my knowledge. In fact, the overview books typically do not even mention Doppler effects in electron waves. Why has the topic been dropped? Möllenstedt's results, although of extremely low velocities, seemed to be encouraging. Maybe the lack of interest is because of the almost exclusive attention paid to image improvement via holography, along with the lack of compelling experiments to do with velocimetry at the time. The experimental front has changed with the advent of micro- and nano-machines, where dynamic effects are critical and nano-material design, where knowledge of dynamic property changes may be helpful. We now have a compelling need for reviving and perfecting velocimetry at these scales. This paper seeks to outline, from the beginning theoretical basis of de Broglie waves, the reasonableness and the mathematics required for Doppler velocimetry. Quantum mechanical arguments are discussed briefly in this paper that may make Doppler shifting impossible with matter waves. Analogies with dynamic optical holography, or fringe counting, and Doppler frequency measurements are detailed—that I believe are directly applicable to electron Doppler measurements as demonstrated by Möllenstedt and Lichte. In addition, some ideas on experiments that may be conducted are outlined with example calculations to prompt discussion and ideas about applications of DEV.

2. WAVE NATURE OF ELECTRONS (PARTICLES

2.1. de Broglie Waves

In 1924, Louis de Broglie postulated that if light was a particle (a photon), then maybe electrons can be viewed as waves. Indeed, any particle (defined as a thing with mass) has a wave description, although for large (heavy) objects, it is infinitesimally small and not observable. Large is a bit of a euphemism; large for these purposes is really anything larger than an electron, proton, neutron, or atom. For background purposes, I trace the development of the de Broglie hypothesis with the relevant equations, beginning with the relativistic definition of momentum [15]:

$$p = \frac{mv}{\sqrt{1-\frac{v^2}{c^2}}}, \tag{1}$$

where m is the mass of the particle and p is the momentum. The relativistic momentum is used because when dealing with particles, typically the particle speeds (v) that appear can be extremely high, approaching the speed of light (c). Note that if $v<<c$, the equation reverts to the nonrelativistic form $p=mv$. Using the definition of force as $F=dp/dt$, and taking the partial derivative of the relativistic momentum equation (1), holding the mass constant, F may be defined as:

$$F \equiv \frac{dp}{dt} = \frac{d}{dt}\frac{mv}{\sqrt{1-\frac{v^2}{c^2}}} = \frac{m(dv/dt)}{\left(1-\frac{v^2}{c^2}\right)^{3/2}}. \tag{2}$$

The work can then be calculated using the following equation:

$$W = \int_{x1}^{x2} F dx = \int_{x1}^{x2} \frac{dp}{dt} dx. \tag{3}$$

F may be substituted into the work equation to yield:

$$W = \int_0^v \frac{m(dv/dt)vdt}{\left(1-\frac{v^2}{c^2}\right)^{3/2}} = \int_0^v \frac{mv}{\left(1-\frac{v^2}{c^2}\right)^{3/2}} dv = \frac{mc^2}{\sqrt{1-\frac{v^2}{c^2}}} - mc^2. \tag{4}$$

Work by definition equals the change in kinetic energy, and realizing that the initial kinetic energy at rest is zero ($v = 0$ in the integration), the kinetic energy can then be expressed as

$$K = \frac{mc^2}{\sqrt{1-\frac{v^2}{c^2}}} - mc^2. \tag{5}$$

At nonrelativistic speeds, this of course reduces to the well-known $K=1/2mv^2$ (using a binomial expansion on the denominator). It is useful to express this in terms of energy, where the total energy equals the kinetic energy plus the rest energy. The rest energy is defined by the famous $E_o=m_oc^2$, the total energy then equals:

$$E = K + m_o c^2 . \tag{6}$$

Equation (6) combined with equation (5), can then be simplified to yield the total energy of the electron:

$$E = \frac{m_o c^2}{\sqrt{1-\frac{v^2}{c^2}}} . \tag{7}$$

This can be solved for the velocity of the electron:

$$v = c\sqrt{1-\frac{m_o^2 c^4}{E^2}} . \tag{8}$$

To express this equation in terms of momentum, $p=mv$ may be substituted on the left side of the equation and also noting that $E=mc^2$, this may be rearranged to be

$$p = \frac{1}{c}\sqrt{E^2 - c^4 m_o^2} . \tag{9}$$

This can be rearranged in terms of total energy to be:

$$E^2 = p^2 c^2 - m_o^2 c^4 . \tag{10}$$

To reach the final goal of calculating the wavelength (λ) of the electron, the use of Planck's concept of the quantization of energy is required. His basic theory, based on the empirical study of blackbody radiation, concluded that matter emitted energy in discrete quanta. In mathematical terms,

$$E = hf = \frac{hc}{\lambda}, \tag{11}$$

where the λ is the wavelength and h is Planck's constant. The momentum can be written as

$$p = \frac{E}{c} . \tag{12}$$

By combining equations (11) and (12), we have the famous de Broglie relationship between momentum and wavelength [16]:

$$p = \frac{h}{\lambda} = \hbar\vec{k} . \tag{13}$$

Where $\vec{k} = 2\pi/\lambda$ is the wave number, or if dealing with a wavefront, the wavevector as expressed in this equation, and $\hbar = h/(2\pi)$. Simply substituting this into equation (9) yields the wavelength in terms of the total energy and some constants:

$$\lambda = \frac{hc}{\sqrt{E^2 - m_o^2 c^4}} . \tag{14}$$

This is a compact equation, but with some simplification, it can be made more useful for calculating the wavelength of electrons in a typical microscope application. The total energy is a combination of the kinetic energy and the rest mass. The kinetic energy of an electron in a microscope results from the acceleration potential applied. The force applied to the electron via the electric and magnetic fields is supplied by the electron gun and optics. The Lorentz force as experienced by the electron is expressed as

$$\vec{F} = -e(\vec{E} + v \times \vec{B}) . \tag{15}$$

This equation expresses the force, F, applied to the electron (e) by the combined magnetic and electric fields ($\boldsymbol{B}$ and $\boldsymbol{E}$). The cathode supplying the electrons is typically maintained at some negative potential, and the anode is maintained at zero potential. With no magnetic field applied, the work required to accelerate the electron from a kinetic energy of zero to some velocity is calculated using the line integral of the electric field and the potential change through which the particle was moved [17].

$$K = e \int_{Anode}^{Cathode} \vec{E} \cdot ds = eU . \tag{16}$$

This states that the kinetic energy is a function of only the accelerating potential in volts (U) through which it travels, irrespective of path. This gives us an equation of total energy, which is, again, the kinetic energy plus the rest mass of the electron:

$$E = K + m_o c^2 = eU + m_o c^2 . \tag{17}$$

Combining equations (17) and (14), and using the standard numbers for the constants e, h, c, and m_o, the following equation can be obtained relating the electron wavelength to the accelerating potential of the microscope [18]:

$$\lambda = \frac{1.226}{\sqrt{U\left(1 + 0.9788 \times 10^{-6} U\right)}} \text{ (nm)} . \tag{18}$$

The previous arguments were developed with relativity in mind. For many applications of electron microscopes, with accelerating voltages below 100 kV, a much simpler expression can be utilized by neglecting the relativistic mass, with at most a 5% error. The following equation expresses the development and final equation for wavelength as a function of accelerating potential U (volts):

$$\lambda = \frac{h}{p} = \frac{h}{m_o v} = \frac{h}{\sqrt{2 e m_o U}} = \frac{1.226}{\sqrt{U}} \text{ (nm)} . \tag{19}$$

2.2. Interference of Particles (or are they waves?)

The de Broglie wave has now described the motion of everyday particles as waves, or maybe more accurately, wave packets. In everyday physics, this applies to light by means of the photon concept, which being both a boson and massless has some properties that heavier particles do not exhibit. Electrons, protons, and neutrons are examples of particles that are regularly available and accelerated to different velocities and, hence, have different wavelengths. The concept of Doppler shifting, required for velocity measurements, could use any of these three particles for this purpose. Currently, the focus is on electrons, as there is a ready source of accelerated and focused particles for use and the concurrent measurement systems in place to measure them. Having noted the wavelength of the particle-wave, a stationary wave propagating in the z-direction can be described with the wavefunction (Ψ):

$$\psi(x,t) = A\cos(\vec{k}\cdot\vec{r} - \omega t) = A\cos\left(\frac{2\pi}{\lambda}x - 2\pi f t\right), \tag{20}$$

where $\vec{k}\cdot\vec{r}$ is the direction vector and distance traveled by the wave. For a single wave traveling in the *x*-direction, it simplifies to the second equation. The frequency is *f,* and/or alternately the rotational rate is ω. The analogy of matter waves with photons is useful but not completely accurate. One fundamental difference is from the idea of the light quantum $E\lambda=hc$, which is a clearly defined attribute of the emission of the photon and completely defines its wavelength and energy. For electron waves, this is not the case. The wavelength, as seen explicitly in equation (18), is also a function of the electric and the magnetic potential the electron wave travels through via the Lorentz force. For electron waves, the frequency and the wavelength are both functions of position and are more properly expressed as

$$\psi(x,t) = A\cos\left(2\pi\left[\int_{x_o}^{x}\frac{1}{\lambda(x)}dx - f(x)t\right]\right). \tag{21}$$

This is because the wavelength and frequency can be modified by passing through an electric or magnetic field and are not uniquely defined properties of the electron wave. This is not critically important as the wavelength and frequency are not directly observable properties anyway [17]. This fact, however, is not important and may seem odd at any rate as diffraction patterns are clearly seen in TEM work—and leads directly to the conclusion that electron waves can interfere even if their wavelengths are not clearly defined. This is because, fundamentally, interference is the measurement of the change of phase ($\Delta\phi$) as two waves travel through space and are recombined; or it is, alternately, the interference of two point sources at the detector as seen in Figure 1.

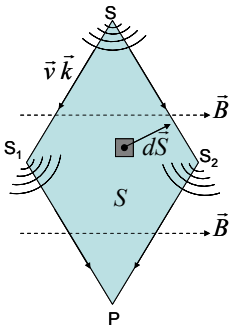

Figure 1. Point source interference model.

The momentum in the presence of the electrostatic and magnetic fields is typically thought of as acting on particles but can be generalized in wave behavior to a phase-shift. This phase shift can be found by integrating around the path SS_2PS_1S, as shown in

$$\phi_2 - \phi_1 = \int_S^{S_2} \vec{k} \cdot d\vec{r} + \int_{S_2}^{P} \vec{k} \cdot d\vec{r} - \int_S^{S_1} \vec{k} \cdot d\vec{r} - \int_{S_1}^{P} \vec{k} \cdot d\vec{r} \,, \tag{22}$$

using the canonical expression for momentum, which includes Maxwell's magnetic field term:

$$\vec{p}' = mv - e(\nabla \times \vec{B}) = \hbar \vec{k} \,. \tag{23}$$

Substituting equation (22) into equation (23), and simplifying via the Stokes theorem, an equation expressing the phase change of the electron wave as it passes through the sample can be found. Alternately, these equations can be derived from the Schrödinger equations, and using the WKB (Wetzel, Kramers, Brillouin) approximation for weak fields, the following phase shift equation can be formulated:

$$\phi_2 - \phi_1 = \frac{1}{\hbar} \oint \left(mv - e(\nabla \times \vec{B}) \right) \cdot d\vec{r} \,. \tag{24}$$

The line integral is carried out along the closed path of the interfering electrons (i.e., along SS_2PS_1S). Separating out the magnetic and electrostatic effects—the equation can be more easily understood as

$$\phi_2 - \phi_1 = \frac{1}{\hbar} \oint mv \cdot d\vec{r} - \frac{e}{\hbar} \int_S (\nabla \times \vec{B}) \cdot d\vec{R} = \frac{2\pi}{h} \oint mv \cdot d\vec{r} - \frac{e}{\hbar} \phi_m \,. \tag{25}$$

Inspecting equation (25) in light of equation (13), we can see that the relation $\vec{k} = p/\hbar = mv/\hbar$ remains valid even with the wavelength ambiguity discussed previously. This is true even in the presence of a magnetic field, which simply adds an offset ϕ_m to the phase change. This returns us naturally to equation (20), the wave equation for an electron. For typical interference work, this equation simplifies to

$$\psi = Ae^{j\left(\frac{2\pi}{\lambda}x\right)} = Ae^{j2\pi\vec{k}\cdot\vec{r}} = Ae^{j\vec{k}\cdot\vec{r}} \,, \tag{26}$$

showing both the trigonometric and complex notation formulation in simplified single wave format and vector format. Complex notation is often used in optics because of the simplification of some of the [19] mathematics, where j is the imaginary number operator $\sqrt{-1}$.

That holography works with electrons is not under dispute and has been demonstrated for many years. Because of coherence issues, the Möllenstadt electron biprism (Figure 2) is the standard interference arrangement for TEM and is briefly explained here as an example of the interference of particle beams.

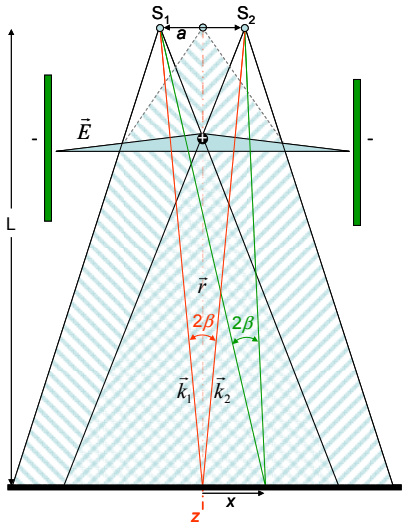

Figure 2. Electron biprism.

The biprism is so termed because of its relation to the Fresnel optical biprism interference experiments. The biprism is one of a number of simple wavefront splitting interferometers that in essence creates two point sources in space from a single source. Young's double-hole experiment is the most famous example of this, but it also includes Lloyd's mirror, incidence at an angle, and reflection and transmission from/through a dielectric layer. These arrangements help ensure the temporal and spatial coherence of the overlapping beams and hence their interference by creating virtual sources from a single source. In fact, these arrangements can be used to test the coherence length by means of changing the path lengths and observing the fringe pattern. Using the illustration in Figure 2, the two virtual sources S_1 and S_2 emit waves that are deflected and added together:

$$\psi_T = Ae^{j\vec{k}_1\cdot\vec{r}} + Ae^{j\vec{k}_2\cdot\vec{r}}. \tag{27}$$

Adding the two wavefronts together as shown above and then multiplying by the complex conjugate gives the irradiance, which is the value measured at the detector:

$$I = \mathrm{Re}(\psi_T{}^*\psi_T) = \mathrm{Re}\left\{(Ae^{j\vec{k}_1\cdot\vec{r}} + Ae^{j\vec{k}_2\cdot\vec{r}})(Ae^{-j\vec{k}_1\cdot\vec{r}} + Ae^{-j\vec{k}_2\cdot\vec{r}})\right\}. \tag{28}$$

Multiplying out, using Euler's equation and a trigonometric identity, the intensity as a function of the distance along the screen can be obtained:

$$I = \mathrm{Re}\left\{Ae^{j(\vec{k}_1\cdot\vec{r}-\vec{k}_2\cdot\vec{r})} + 2A\right\} = \mathrm{Re}\left\{2A\cos(\vec{k}_1\cdot\vec{r}-\vec{k}_2\cdot\vec{r}) + 2A\right\} = 4I_o\cos^2\left(\frac{\vec{k}_1\cdot\vec{r}-\vec{k}_2\cdot\vec{r}}{2}\right). \quad (29)$$

The direction vectors shown in Figure 2 work out to be

$$\vec{k}_1 = |k|\sin\beta\vec{u} + |k|\cos\beta\vec{w}, \vec{k}_2 = -|k|\sin\beta\vec{u} + |k|\cos\beta\vec{w}, \vec{r} = x\vec{u} + z\vec{w}, \quad (30)$$

$$\vec{k}_1\cdot\vec{r} - \vec{k}_2\cdot\vec{r} = 2kx\sin\beta \approx 2kx\beta. \quad (31)$$

This makes the final intensity profile over the viewing screen to be

$$I(x) = 4I_o\cos^2\left(\frac{2\pi\beta x}{\lambda}\right). \quad (32)$$

In the biprism arrangement, one side of the beam may be passed through a sample, which then causes some phase shift in the wavefront, and then it is recombined with the reference wave to create an interference pattern. Information about the sample is obtained by measuring the phase change, $\Delta\phi$. This, of course, is subject to a number of constraints, including the inherent coherence, both spatial and temporal, of the electron beam. In addition, the elastic and inelastic interactions of the electron with the sample affect the fringe contrast. Both types of scattering have been shown to interfere; however, beam energies must be matched between the reference and object beam by causing both to travel through a scattering medium as demonstrated in a number of electron holography papers [20,21,22].

2.3. Spatial and Temporal Coherence and Limitations on Holography

Coherence has two components, both of which are important for the discussion of electron holography. They are spatial and temporal coherence (often expressed as transverse and longitudinal, that is, waves that vibrate in unison for a long period of time over a wide space [23]). Thinking about coherence in terms of Young's double slit experiment is useful to give a physical feel for the coherence limits required for fringe formation. The wave packet's coherence must be wide enough spatially to cover both holes (or *a* in the biprism discussion) and long enough to cover the path length change. Both concepts are illustrated in Figure 3. Coherence description, with (a) Young's slit experiment [10], and (b) path length illustration [24].

.

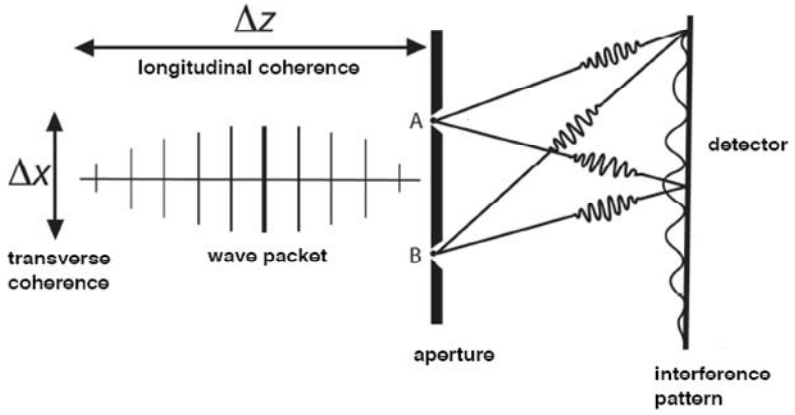

(a) (b)

Figure 3. Coherence description, with (a) Young's slit experiment [10], and (b) path length illustration [24].

Fundamentally, coherence can be thought of as the relationship of the wavefront in a given wave packet. The temporal coherence is determined by the energy spread of the beam, and the spatial coherence upon the uniformity of the phase front at some point in space. Temporal coherence indicates how long a wavefront remains sinusoidal and here is expressed as a distance (Δz). This is dictated by the finite length of a wave packet and is related to the emission time $\Delta\tau$ of the electron wave. For light, the temporal coherence length Δz is dictated by the emission time and the velocity c in the case of light:

$$\Delta z = v\Delta\tau \,. \tag{33}$$

For light, with emission times on the order of $\Delta\tau \cong 10^{-8}$ s, this typically leads to meters of coherence length. For electrons, $\Delta\tau$ is estimated from the Heisenberg uncertainty relation:

$$\Delta E \Delta\tau \cong h \,, \tag{34}$$

$$\Delta z = \frac{\lambda^2}{\Delta\lambda} = \frac{2E}{\Delta E}\lambda \,, \tag{35}$$

where ΔE is the energy spread of the electron gun, typically 1 eV, and gives a $\Delta\tau \cong 10^{-15}$ s. At 100 kV, the coherence length is 680 nm or in waves, 2×10^5 λ [17]. The theoretical temporal coherence lengths were confirmed experimentally by applying a known phase offset to one leg of the electron biprism and observing when the fringes disappeared. The total phase shift found is a measure of the coherence length. This was done by Möllenstedt [25] using a Wien filter and by Schmid [26] using metallic tube held at a constant voltage to supply a phase change to the beam. Table 1 shows typical coherence lengths at 100 kV for a range of energy spreads from the source (ΔE).

Table 1. Temporal (longitudinal) coherence length.

U (kV)	ΔE (eV)	Δτ (s)	v (m/s)	Δz (nm)
100	3	1.38E-15	1.64E+08	227
100	2	2.07E-15	1.64E+08	340
100	1	4.14E-15	1.64E+08	680
100	0.5	8.27E-15	1.64E+08	1359
100	0.1	4.14E-14	1.64E+08	6797

The spatial or transverse coherence (Δx) is related directly to the electron source size (b) via the van Cittert-Zernike theorem [27]:

$$\Delta x = \frac{L\lambda}{b}, \tag{36}$$

referring back to Figure 2 for the definition of L. Basically, the smaller the source tip b, the better the spatial coherence. Modern electron emission tips are on the order of angstroms and yield spatial coherence that completely fills the condenser aperture, and even the fully focused spot on the specimen is coherent [19,28].

This page intentionally left blank.

3. ANALOGY TO OPTICAL TEMPORAL HOLOGRAPHY

3.1. Introduction to Optical Analogy

Electron Doppler holography looks to measure the frequency shift of the electron wave and from that to infer the velocity (or dynamically changing magnetic or electric field) of the sample. As mentioned previously, the electron wave frequency is not measurable because of its extremely high frequency. This is also true of optical frequencies. Doppler measurements are successfully made via homodyning or heterodyning the optical frequencies down to measurable rates via a wavefront splitting interferometer, typically a Mach-Zehnder arrangement. How this might be applicable to electron beams may be thought of via the concept of fringe counting. This can be understood by thinking of the fringe pattern created by the sample, moving across the detector as the phase is dynamically changed. For example, a changing magnetic field causes the phase to be shifted, and if this is done slowly, a series of fringe patterns results that can be recorded. If a sensor is placed at a single location, a sinusoidal intensity variation results. This single detector can typically be much faster and more sensitive than a CCD camera, and this yields benefits in terms of speed of response to the changing intensity. It is, however, not intuitively obvious that Doppler and fringe counting are identical [29], and the next sections mathematically reconcile the two concepts, via optical example and analogy, that is, the "dynamic hologram" and the laser Doppler vibrometer.

3.2. Reconciling Temporal Holography and Doppler – the General View

Using a standard Michelson interferometer (a wavefront splitting interferometer like the electron biprism) rather than the Mach-Zehnder setup that is more typically used for LDV arrangements, the mathematics of both dynamic holography and Doppler velocimetry are outlined and reconciled. Some complications of each technique that increase their sensitivity or usefulness and have become standard are overlooked in this presentation for the sake of simplicity. These complications include frequency shifting used in LDVs for velocity direction determination, phase shifting used in dynamic holography to determine sub-wavelength deformations, and any imaging optics utilized will be neglected. The following derivation uses the Michelson interferometer setup shown in Figure 4. The laser source is split by the beamsplitter and illuminates both an object and reference surface. It should be noted that in this setup, because of the return path length, a factor of 2 shows up in both velocity and phase measurements as noted in the discussion. This arrangement has been accomplished with an electron beam by Lichte and Möllenstedt [30]. Measurement of the velocity or deformation of the object may then be made by processing the resulting time varying intensity measured by the detector. For LDVs, the detector is typically a fast photodiode rather than a camera because of the relatively high frequencies of the Doppler signal (typically kHz or MHz) and yields a single measurement location of velocity.

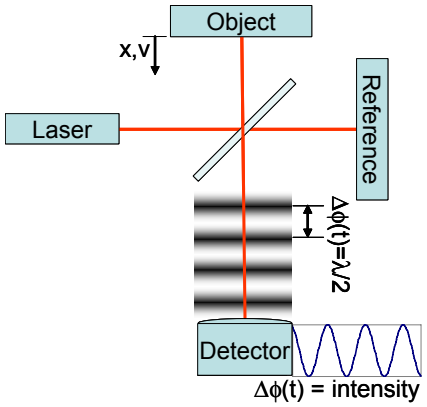

Figure 4. Michelson interferometer.

The electromagnetic equations using complex notation of the light coming from the laser can be described by

$$E(t) = \mathrm{Re}\left\{Ce^{j\omega t}\right\}. \tag{37}$$

The Real operation will be omitted from this point on and should be assumed by the reader as is typical for this type of derivation. The frequency of the light is expressed by ω, time is t, and C is the amplitude of the signal. This notation is greatly simplified from the entire vector equation shown as a complete description in many sources [31] but is correct for the uniform distribution with a planar wavefront in a single direction found in the Michelson interferometer. After reflecting from the surface of the object, the light beam is

$$E_O(t) = Ae^{j(\omega_o t + \phi_o(t))}, \tag{38}$$

where A is the amplitude after reflecting from the object and returning through the beamsplitter, ω_o is the Doppler shifted frequency, and ϕ_o is the phase shift from the object. Strictly speaking, the phase shift is a function of both space and time. This x, y dependence has been dropped and can be thought of as being equivalent to looking at the information for a single pixel or photodiode. The equation describing the reference beam after returning through the beamsplitter is

$$E_R(t) = Be^{j(\omega t + \phi_r)}, \tag{39}$$

where B is the amplitude after returning from the reference through the beamsplitter, ω is the optical frequency, and ϕ_r is the phase shift from the reference surface. Upon combining the two beams at the detector, the total electromagnetic radiation is

$$E_T(t) = Ae^{j(\omega_o t + \phi_o(t))} + Be^{j(\omega t + \phi_r)}. \tag{40}$$

Detectors (photodiodes and digital cameras) respond to intensity (irradiance) of the signal, which is defined as the square of the electromagnetic amplitude:

$$I(t) = E_T E_T^*, \tag{41}$$

where E^* represents the complex conjugate. Multiplying this out and noting that there are no complex portions to the constants A and B result in the following intensity measured at the detector:

$$I(t) = A^2 + B^2 + 2AB\left(e^{j[(\omega-\omega_o)t+(\phi_r-\phi_o(t))]} + e^{-j[(\omega-\omega_o)t+(\phi_r-\phi_o(t))]}\right), \tag{42}$$

or simplify the constants of equation (6) to a single I_o and convert to the more familiar trigonometric description:

$$I(t) = I_o + D\cos\left[(\omega-\omega_o)t + (\phi_r - \phi_o(t))\right], \tag{43}$$

where the phase change is often defined as $\Delta\phi = \phi_r - \phi_o(t)$. This equation is both the Doppler and ESPI description of the light, depending on how the two terms in the cosine function are defined, but if inspected closely, the reader may notice some mathematical legerdemain. That is, a time varying phase is by definition the instantaneous frequency, and therefore the ω terms and the ϕ terms are redundant in this presentation. However, for purposes of illustration, if quasistatic is assumed ($\omega = \omega_o$), the Doppler term goes to zero, leaving the traditional holographic formulation; or if one assumes that $\Delta\phi$ is not a function of time, it becomes a constant, yielding the typical Doppler formulation. Both descriptions are appropriate and physically identical to the sinusoidal intensity change experienced as the fringes are seen moving over a pixel in time varying holography, or fringe counting in LDVs. This explanation is expanded and enhanced in the following sections by starting from the traditional holography formulations and Doppler formulations separately and reconciling them.

3.3. Approach Using Temporal Holography Notation

Approaching the reconciliation via dynamic holography notation [32], the following equation contains the standard description of the light intensity on a given pixel:

$$I(t) = I_O\left[1 + \gamma\cos\left(\phi_r - \phi_o(t)\right)\right], \tag{44}$$

where I_o is the DC intensity averaged on the detector from the high-frequency optical terms, ϕ_r is the reference beam phase, γ is the modulation constant, and $\phi_o(t)$ is the phase change caused by the object motion. All three variables are of course functions of x and y in the camera image, but simplified to a single pixel for this formulation. In the setup in the Michelson interferometer, the object motion causes a phase change in $\phi_o(t)$:

$$\phi_o(t) = \frac{2\Delta x(t)}{\lambda}. \tag{45}$$

A deformation of Δx in a given time, Δt, of course, can be expressed as a frequency:

$$f = \frac{2\Delta x(t)}{\lambda t} = \frac{2v}{\lambda}, \tag{46}$$

where the motion in a given time is merely velocity v. The final equation (46) is the Doppler frequency change because of the object velocity. With equations (45) and (46), a final description of a time varying holography signal is

$$I(t) = I_O\left[1 + \gamma\cos\left(\phi_r - \frac{2v}{\lambda}t\right)\right] . \tag{47}$$

3.4. Approach Using Doppler Frequency Shift Notation

Approaching the derivation from LDV terminology is slightly different and begins with the Doppler frequency shift description for light. An assumption made here that the surface velocity is much smaller than the speed of light simplifies the relativistic effects. Referring again to the Michelson interferometer, the velocity of the object surface can be shown to cause a frequency shift in the impinging light of [33]:

$$f_o = \frac{f}{1 - \frac{2v}{c}} , \tag{48}$$

where v is the velocity of the object, f is the optical frequency, f_o is the Doppler shifted frequency caused by the object motion, and c is the velocity of the light in air (for this case). When the beam is mixed with another beam of the same frequency (as in the Michelson interferometer), the resulting heterodyne term, $\Delta\omega$ or $\Delta\phi$, as described in equation (7) becomes

$$\Delta f = f_o - f = f\left(\frac{1}{1 - \frac{2v}{c}} - 1\right) = f\left(\frac{2v}{c - 2v}\right) . \tag{49}$$

If we assume that $c>>v$ and that $f=c/\lambda$, the equation can be simplified to

$$\Delta f = f_o - f = \frac{2v}{\lambda} \Rightarrow f_o = f + \frac{2v}{\lambda} . \tag{50}$$

By plugging this into equation (43) and using $\omega=2\pi f$, the following equation is found:

$$I(t) = I_O + D\cos\left[\Delta\phi - \frac{2v}{\lambda}t\right] . \tag{51}$$

If a few constants are rearranged, this equation is identical to equation (47) in the dynamic holography development.

3.5. Analogy Conclusions

It is apparent from the above derivations that temporal holography and Doppler are equivalent, and are two ways of looking at the same phenomenon. Probably the most intuitive way of visualizing it is to think of an imaginary fringe field in front of the detector (as shown in the Michelson interferometer) that moves proportionally to the object surface. As the surface moves forward, the fringes will alternate from light to dark, creating a sinusoidal waveform on the detector as a function of time. Depending on whether you are looking at the fringes passing by (fringe counting) or the frequency at which they pass by (Doppler), you get different information—namely displacement or velocity.

4. THE DOPPLER EFFECT ON ELECTRONS

4.1. Detailed Discussion of a Doppler Electron Experiment

Because the work of Möllenstedt and Lichte is so important to the proof of this concept, the work presented in their paper [13] is briefly discussed here. A biprism was used to split the electron beam into two beams, *r* and *o*, as indicated in Figure 5. A magnetic prism was used to deflect the beams onto an electron mirror. The mirror was a conducting surface held at a potential with an anode in front of it. This electron mirror was then rotated by means of a piezo crystal with an applied time-varying voltage, which increased the velocity of one beam and decreased the velocity of the other. The beams were sent back through the magnetic prism and recombined via a second biprism to interfere them. This setup was exactly equivalent to the Michelson interferometer discussed in the optical analogy, and they proposed an equivalent equation to the Doppler shift equation (51) derived previously. They showed a set of time varying fringes as in Figure 5c. They put a slit detector at a single location under the screen and measured the Doppler beat via the intensity measured by the detector. The *U* plot indicates the voltage applied to the piezo, with the positive slope imparting a Δv = 60 pm/s, and the negative slope Δv = 66 pm/s. The corresponding beat frequencies are 0.92 Hz and 1.02 Hz, within 10% of the calculated theoretical Doppler beat. This is experimental proof that the Doppler electron microscope could be a functional tool.

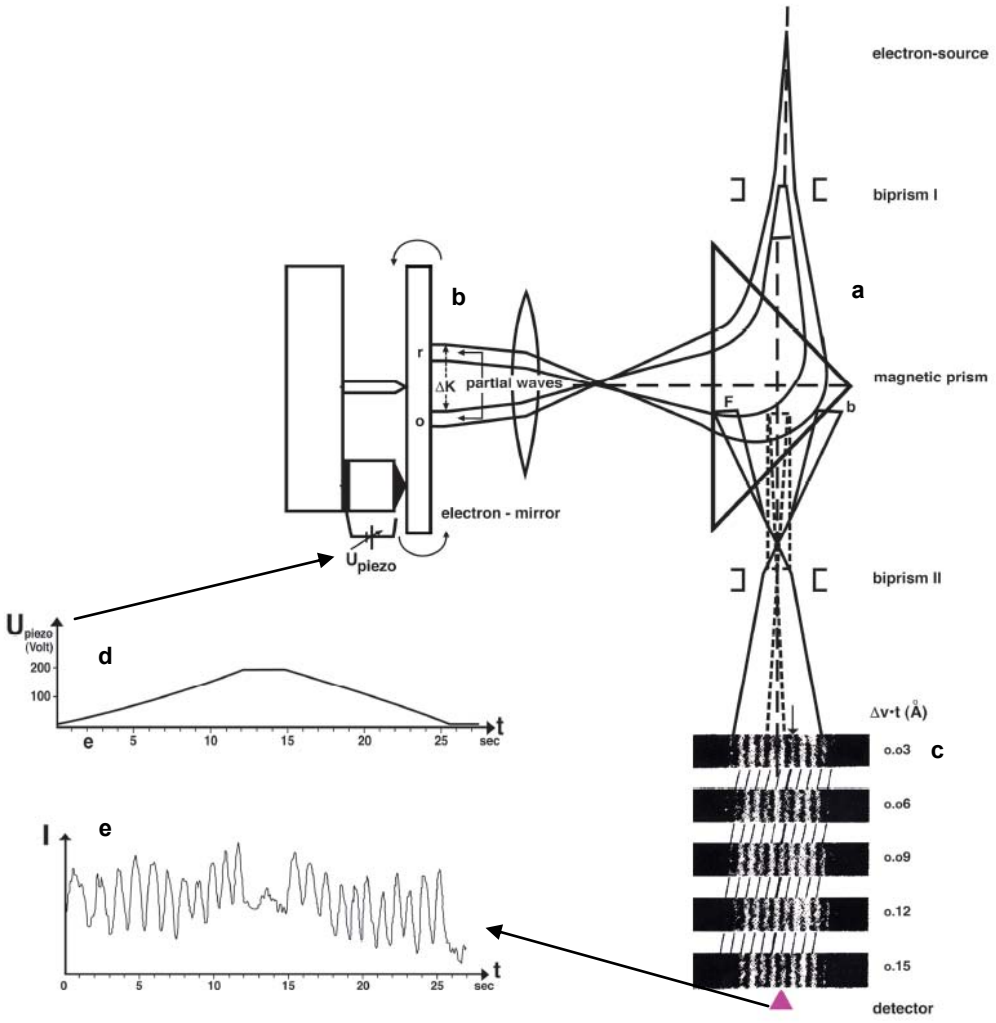

Figure 5. Illustrations from paper.
a) Michelson interferometer, b) electron mirror, c) moving fringes,
d) voltage applied to piezo, and e) Doppler beat because of velocity of mirror.

4.2. The impossibility of Doppler—a Counter Argument (or fly in the ointment)

Although the argument from optical analogy seems compelling, electron waves in many ways (but not all) behave as light waves. Most importantly for our arguments, they diffract and interfere with one another. However, unlike laser light, which may interfere with other photons in the wave-train (there is some discussion whether this is the case), electrons only interfere with themselves. This is because electrons are fermions or particles with half-integer spins and are unable to interfere with each other, whereas photons are bosons, and this exclusion is not required. This means that the electron fringe patterns detected are statistically built up over a few seconds rather than instantaneously. The time to form this statistical picture is dependent on the beam current, or number of electrons per second hitting the detector. With higher beam currents fringes could form "instantaneously" as compared with the sampling time.

Beyond the time for fringe formation, three other potential counter arguments to my electron Doppler hypothesis are presented by F. Zhou in his paper regarding the interference of inelastically scattered electrons, where he states that moving fringes are impossible with electron beams [34]. The arguments presented in the paper involve three main points: electrons with energy changes that are "too large" cannot interfere, the phase incoherence of the source precludes moving fringes, and the inelastic scattering in matter puts the electrons in quantum mechanically orthogonal states that cannot interfere. From my reading of the literature, there is not a complete agreement with his main thesis, and various counter arguments have been proposed. I summarize these arguments here, starting with the energy change argument. Zhou states that an energy change greater than 10^{-15} eV would create rapidly moving interference fringes that are unobservable with typical sensors. For example, inelastic scattering creates energy changes on the order of 0.1 eV to 2 keV, which would make the recording time too short to be practical. Interestingly, Zhou's cutoff energy of 10^{-15} eV is approximately the energy change measured by Möllenstedt and Lichte in their Doppler experiment (i.e., $E=hf_{Doppler} \cong 4\times10^{-15}$ eV). A further detail for the electron Doppler measurements is that the electrons are not inelastically scattered. They still do, however, experience an energy change (i.e., $\delta E=hf$). Van Dyck et al. [21] discuss theoretical values for allowable energy change for interfering electron beams and develop from quantum mechanical arguments the following equation:

$$\left|E_0 - E_1\right| = \delta E < \frac{h}{t}, \tag{52}$$

where t is the record time and h is Plank's constant. Values of prospective Doppler energy changes and sampling times are summarized in Table 2.

Table 2. Sampling rates for different Doppler energy shifts.

Record t (s)	$\Delta E < h/t$ (eV)	f_{sample} (MHz)
1	4.14E-15	0.000001
0.1	4.14E-14	0.00001
0.01	4.14E-13	0.0001
0.0001	4.14E-11	0.01
0.00001	4.14E-10	0.1
0.000001	4.14E-09	1

Van Dyck's interference arguments are most easily visualized by comparing the energy spread of the source, and the energy change caused by the frequency shift of the electron beam. This is shown in Figure 6, where δE is the energy shift because of scattering, and ΔE is the energy spread of the source. Graphically, their argument is summarized by saying that as long as the two beam energies overlap, there will be interference. Other researchers have drawn similar conclusions, both theoretically and experimentally [20,22,35]. For realistic Doppler sampling times of 1 MHz (as seen in Table 2), this would imply a possible maximum energy change of 10^{-9} eV, well within the energy spread of a typical source, and yielding realistic velocity measurements as will be outlined later in this paper. One last point regarding energy change and interference comes from the analogy to light interference, where with even quite large energy changes (i.e., frequency changes) the photons still successfully interfere.

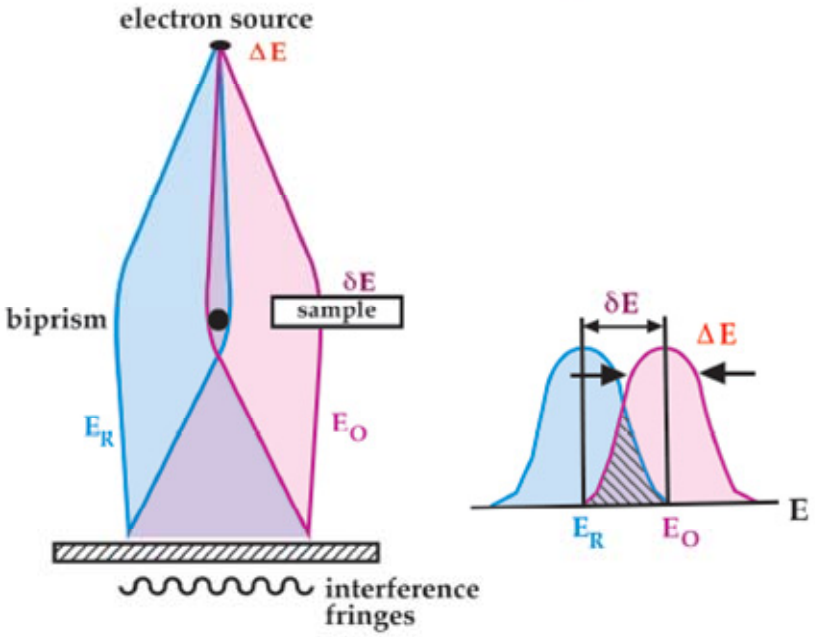

Figure 6. Schematic of the energy spread and the effect on interference [21].

Zhou next makes the argument that electron sources are phase incoherent; that is, each electron, regardless of whether the energy and wavelength are equal, has a different phase. In the optical analogy, this is equivalent to a well-filtered light source, like an arc lamp. He argues that the wave functions only describe the behavior of a single electron—and hence, moving fringes cannot be observed in an electron microscope. As a counter argument to this, I return to the optical domain, where the first interference experiments were conducted with just such a phase incoherent but wavelength filtered light source. Arguing from the same concept of a finite wave-packet (photon) with incoherent phase, Hecht [16] demonstrates that phase incoherence does not matter for the interference of the packets as long as there is frequency stability (i.e., a small energy spread ΔE, as argued previously). An example of this phenomenon comes from the author's work with laser speckle fields used for Doppler vibrometry, where many laser speckles (1000s), all with random phases relative to each other, are combined on a single detector. This summation of random phases still yields a measurable Doppler frequency on the photodiode. This is analogous to a large number of random phase electrons interfering, and through a random walk argument, still yielding measurable Doppler frequencies.

Zhou's final argument is that elastically scattered electrons, if they have different energies, are incoherent because of them being quantum mechanically orthogonal to one another. I have no counter arguments from electron holography; however, this argument certainly does not apply in the optical domain. This would make traditional LDVs nonfunctional, as the Doppler shift is also an energy shift via $E=hf$ as discussed earlier—and we know from practice that it does work.

In summary, comments regarding moving fringes seem overstated, as researchers using electron holography have observed moving fringes at video rates anyway [36], and so the scale of the rate must obviously be important. Can you have a faster detector or larger beam current and hence see faster moving fringes? I would argue that you can. There also seems to be some disagreement with Zhou's conclusions regarding inelastic scattering, as outlined in a number of papers already summarized or referenced in this review.

This page intentionally left blank.

5. PRACTICAL CONSIDERATIONS FOR THE DEV

5.1. Introduction to the DEV

Even if the theoretical considerations indicate that Doppler electron velocimetry should work, this does not indicate whether the sources, fringe formation time, sensor sensitivity, and realistic experimental energy changes work out to a practical instrument. For a thought experiment on the applicability of this concept to a real measurement, I use the concept of a shearing velocimeter and a typical MEMS cantilever beam in an electron mirror configuration similar to the work by Möllenstedt and Lichte. To begin the practical discussion, Table 3 shows the range of wavelengths available in typical TEMs and their accelerating voltages. The main strength of the Doppler electron approach is the extremely short wavelengths as clearly illustrated in the table, which alleviates the diffraction limitations of optical wavelengths. Even low accelerating voltages lead to sub-nanometer wavelengths. The following sections outline practical coherence values, energy changes, and the shearing DEV.

Table 3. Electron wavelengths and the corresponding acceleration voltage.

U (kV)	λ (nm)	K (1/nm)	me/mo	v/c
0.1	0.12264	8.154	1.00020	0.01978
1	0.03876	25.797	1.00196	0.06247
5	0.01730	57.796	1.00978	0.13887
10	0.01220	81.935	1.01957	0.19498
15	0.00994	100.592	1.02935	0.23711
20	0.00859	116.434	1.03914	0.27186
30	0.00698	143.284	1.05871	0.32837
35	0.00645	155.132	1.06849	0.35227
50	0.00536	186.729	1.09785	0.41268
75	0.00432	231.347	1.14677	0.48948
100	0.00370	270.163	1.19569	0.54822
150	0.00296	338.173	1.29354	0.63432
200	0.00251	398.732	1.39139	0.69531
250	0.00220	454.824	1.48923	0.74102
300	0.00197	507.933	1.58708	0.77652
400	0.00164	608.289	1.78277	0.82787
500	0.00142	703.594	1.97847	0.86286
600	0.00126	795.666	2.17416	0.88795
700	0.00113	885.514	2.36985	0.90661
800	0.00103	973.753	2.56555	0.92091
900	0.00094	1060.785	2.76124	0.93212
1000	0.00087	1146.886	2.95693	0.94108
2000	0.00050	1982.858	4.91387	0.97907

5.2. Important Properties of Available Electron Sources

The field emission gun (FEG) has revolutionized electron holography. It combines two very important attributes of an extremely small emission area and a low energy spread. Table 1 outlines a realistic range of energy spreads of commercially available FEGs from 3 eV to 0.1 eV and their corresponding longitudinal coherence length. These numbers indicate a very usable range of values of nearly 1-micron path length difference between interfering beams. Additionally, the spatial coherence is on the order of hundreds of microns, which allows large areas of the sample to be coherently illuminated. Modern electron guns, in addition to good coherence, are able to supply very high beam currents. Table 4 summarizes the source brightness for various electron sources and their beam currents at the sample.

Table 4. Typical electron source brightness and beam current.

Electron Beam Sources	Required Vacuum (Torr)	Virtual Source Diameter (μm)	Energy Width (eV)	Acceleration Voltage (kV)	Measured Brightness, β (A cm^{-2} sr^{-1}) †	Current Density at Specimen (A cm^{-2}) *
Heated Field Emission	10^{-8}-10^{-9}	0.1	0.8	100	10^{7}-10^{8}	20
RT Field Emission	10^{-10}	0.002	0.28	100	2×10^{9}	4000
Hair-Pin Cathode	10^{-5}	30	0.8	100	5×10^{5}	1
Tungsten (W) Cathode	10^{-6}	10 – 50	1-2	100	1 to 5×10^{5}	3
LaB_6 Cathode	10^{-6}	5 – 10	1	75	7×10^{6}	14

† β in Equation 53. * With 0.8 mrad illuminating aperture (A cm^{-2}). $j_{Specimen}$ in Equation 53.

The current j at the sample can be calculated from the following equation:

$$j_{Specimen} = \pi\beta\theta^2 = \pi\beta\left(\frac{r_{CA2}}{D3}\right)^2, \tag{53}$$

where β is the source brightness in A/cm^2/sr, r_{CA2} is the radius of the condenser aperture, and D3 is the distance to the sample from the aperture. Additionally, the beam current at the image plane can be calculated from

$$j_{image} = \frac{j_{Specimen}}{Mag^2}. \tag{54}$$

For a typical FEG source, A/cm^2 can typically be obtained. When a large magnification is used, this will lead to nAmps at the detection screen, but for the DEV, we are using scanning points, so the entire source current is theoretically available for detection. In taking these numbers along with a typical semiconductor detector response rate of 100 kHz with a beam current of 10^{-11} A [17], there is plenty of dynamic range to work with for making measurements. Even using a traditional fast phosphor screen (P-47 for example) and a photodiode, response times could be achieved in the kHz range rather easily.

5.3. A Shearing DEV Measuring MEMS Beam Vibration

A shearing velocimeter is proposed as a possible "real-life" experimental example. This concept builds on the Doppler experiment of Möllenstedt and Lichte but adds a MEMS component and the idea of shearing velocimetry. The shearing concept allows the maximum velocity difference between the two probe beams to be controlled by controlling how far apart the two beams are—or the shearing distance. The MEMS component is a simple cantilever beam with a thickness of 2 microns and a length of 500 microns. This leads to a typical fundamental frequency of 20 kHz. Both the cantilever beam and the shearing interferometer are shown in Figure 7.

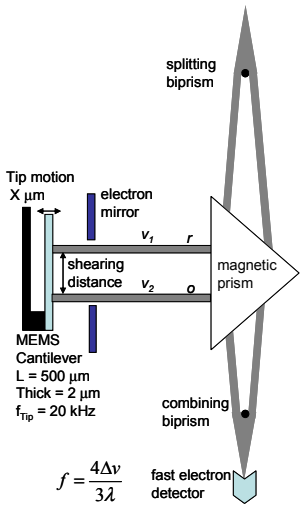

Figure 7. Shearing interferometer and typical MEMS beam.

Assuming a parabolic velocity profile, and making measurements at the tip and a defined shearing distance away from the tip, Doppler frequencies and their concomitant energy change can be calculated. The equations used for these calculations were derived by Sherzer [14]. It should be noted that there is a factor of 4/3 in the equation rather than the typical 2 found previously (Eq. 51), and this is because of the effect of the electron mirror on the motion of the electron beam. The equation that relates the velocity difference between the two beams (Δv) and the Doppler frequency is

$$f_{Doppler} = \frac{\Delta E}{h} = \frac{4\Delta v}{3\lambda}. \tag{55}$$

Using this equation and some proposed tip velocities and shearing distances, Table 5 indicates frequencies and energy shifts that have been calculated based on the beam above. The tip displacement range is varied from 2 microns to 15 pm, which covers the entire range from reasonably large deflections to the thermal excitation of the beam at rest. Doppler frequencies range from 57 MHz to 4 Hz in the table, depending on the tip displacement and the shearing distance. The table indicates that for reasonable tip motions of 10 nm and a shearing distance of 1 micron, the Doppler frequency is 288 kHz—a very reasonable value for measurement with a fast semiconductor device. Another point to note regards the energy change of the beam (ΔE), where for most of the table, the values are much larger than the 10^{-15} eV proposed by some researchers as the theoretical limit, but much less than the typical energy spread of the source (>0.1 eV) proposed as the limit by others. In addition, Table 2 outlines required sampling rates and the related energy changes that are comparable to those in Table 5.

Table 5. Shearing velocity calculations for MEMS beam.

Beam length = 500 μm - Parabolic velocity distribution

λ (nm) 0.0037

Tip (μm)	f_{Tip} (kHz)	Tip v (mm/s)	Shearing (μm)	Δv (mm/s)	Δv (nm/s)	ΔE (eV)	$f_{Doppler}$ (kHz)
2	20	40	1	0.15984	159840	2.382E-07	57600
0.1	20	2	1	0.007992	7992	1.191E-08	2880
0.01	20	0.2	1	0.0007992	799.2	1.191E-09	288
0.001	20	0.02	1	7.992E-05	79.92	1.191E-10	28.8
1.50E-05	20	0.0003	0.01	1.19999E-08	0.012	1.788E-14	0.0043243

This page intentionally left blank.

6. EXPERIMENTAL IDEAS

6.1. Introduction to Experimental Ideas

Is this an instrument in search of a problem? Maybe. Of course, as micro- and nano-machines continue to shrink in size, dynamic measurements will continue to be important for characterizing and testing the designs. It will not be long before current optical techniques will not work—prompting the same transition that has made the electron microscope successful. What could be measured? Typically, any dynamic event on a small scale would be a candidate, including mechanical, electrical, and magnetic events. Here in no particular order are some ideas for developing and applying DEV.

1. Of course, repeating Möllenstedt's work would be a good starting point. This could use a vibrating MEMS component as the electron mirror, with the substrate next to it being the reference surface.
2. If the velocity differential is too great between the reference and object beams of the interferometer, a "shearing" interferometer setup could be used to find the incremental change between two points near one another. Figure 7 shows the conceptual setup of the shearing electron velocimeter. By placing these points arbitrarily close, the velocity gradient can be controlled. Then, by scanning the points, the velocity profile can be built up.
3. An example of time varying magnetic fields is in Curie temperature effects on magnetic fields in metals. A very slow version of this was demonstrated by Hirayama [36].
4. Young's fringe experiment with holes that move would cause moving fringes.
5. Using the biprism and a dynamic electric field in the object path, rather than a sample, could yield a controllable, known dynamic Doppler shift.
6. In the "way in the future" possibilities, the DEV could be used as a data storage device by measuring the Doppler shift of the magnetic field in a recording medium as it traveled under the probe beam.
7. Additional ideas yet to be developed…

6.2. Unknowns and Challenges

At this point in the research, there are two unknowns regarding the potential success of DEV. The first is the coherence length drawbacks of electron microscopy. Work has been ongoing to improve the sources; and I think for preliminary work, current technology is certainly more than adequate. In addition, electron detection equipment is potentially sensitive enough and fast enough to be used for Doppler detection, possibly up to the MHz rate. However, this is dependent on a source that supplies a high enough coherent beam current. While the electron optics such as biprisms and mirrors have been demonstrated, their availability is unknown and most likely will have to be improved to create a high-resolution DEV. Probably the largest unknown is the quantum mechanical aspects of electron interference. Doppler electron research in general is both a challenge and an interesting untested regime for particle wave interference. Can moving fringes be detected? Why or why not? The literature I have found is mixed on this topic, and it seems that interesting physics can be conducted beyond the creation of a practical

electron velocimeter. Another interesting concept is to enforce phase coherence on the electron beam to create an "electron laser." There are some possibilities in this direction by exploiting work done with free electron lasers. The general concept is to use the electric field of a laser beam to bunch the electrons together, enforcing phase coherence [38,39]. If successful, this could potentially help electron holography in general.

7. CONCLUSIONS—IS DOPPLER ELECTRON VELOCIMETRY POSSIBLE?

This question remains unanswered. I think the arguments from optical analogy comparing fringe counting and Doppler, along with demonstrated moving fringes, at least at video frame rates, make the concept a distinct possibility. In addition, the demonstration of electron Doppler shifting, while at an extremely low energy and velocity, is also promising. However, there remain some unanswered physics questions that beg to be researched further.

This page intentionally left blank.

8. REFERENCES

1. Maier-Leibnitz, H., T. Springer, Z. Physik, 167, 368, 1962.
2. Berman, P.L., Editor, *Atom Interferometry*, Academic Press, San Diego, 1997.
3. Gabor, D., "Microscopy by reconstructed wave-fronts," Proc. Roy. Soc. A, 197, 454, 1949.
4. Estermann, I., A. Stern, Z. Physik 61, 95, 1930.
5. Marton, L., Phys. Rev. 85, 1057, 1952.
6. Matteucci, G., "Electron holography used to realize Young's double-hole experiment together with the mapping of magnetic fields," European Journal of Physics, 26, 481, 2005.
7. Möllenstedt, G., H. Düker, Zeitshrift für Physic, 42, 41, 1955.
8. Li, M.C., "A modified Marton-type electron interferometer," Z. Physik B, 29, 161, 1978.
9. Lichte, H., G. Möllenstedt, H. Wahl, "A Michelson interferometer using electron waves," Z. Physik, 249, 456, 1972.
10. Tonomura, A., "Applications of electron holography," Reviews of Modern Physics, 59, 639, 1987.
11. Missiroli, G.F., G. Pozzi, U. Valdrè, "Electron interferometry and interference electron microscopy," J. Phys. E: Sci. Instrum., 14, 649, 1981.
12. Völkl, E., Allard, A.F., Joy, D.C., *Introduction to Electron Holography*, Kluwer Academc/Plenum Publishers, New York, 1999. The first chapter written by Möllenstedt himself describes the development of the biprism.
13. Möllenstedt, G., H. Lichte, "Doppler shift of electron waves," 9th International Congress on Electron Microscopy, Toronto, 1978, pp. 178-179.
14. Scherzer, O., "Der electronenoptische Doppler-Effeckt," Optik, 54, 315, 1979.
15. R.A. Serway, *Physics for Scientists and Engineers, 4th Edition*, Saunders College Publishing, Chicago, 1982 (p. 1173-1175).
16. E. Hecht and A. Zajac, *Optics*, Addison-Wesley Publishing Co., Reading, Massachusetts, 1974.
17. L. Reimer, *Transmission Electron Microscopy*, Springer Series in Optical Sciences, New York, 1984.
18. Z.L. Wang, *Elastic and Inelastic Scattering in Electron Diffraction and Imaging*, Plenum Press, New York, 1995.
19. Völkl, E., Allard, A.F., Joy, D.C., *Introduction to Electron Holography*, Kluwer Academc/Plenum Publishers, New York, 1999. The first chapter written by Möllenstedt himself describes the development of the biprism.
20. Herring, R.A., "Energy-filtered electron-diffracted beam holography," Ultramicroscopy, 104, 261, 2005.
21. Van Dyck, D., H. Lichte, J.C.H. Spence, "Inelastic scattering and holography," Ultramicroscopy, 81, 197, 2000.

22. Lichte, H., B. Freitag, "Inelastic electron holography," Ultramicroscopy, 91, 177, 2000.

23. Cho, B., T. Ichimura, R. Shimizu, C. Oshima, "Quantitative evaluation of spatial coherence of the electron beam from low temperature field emitters," Physical Review of Letters, Vol. 92, 246103, 2004.

24. Lenz, F., Wohland, G., "Effect of chromatic aberration and partial coherence on the interference pattern of an electron biprism interferometer," Optik, 67, 315, 1984.

25. Möllenstedt, G., Wohland, G., "Direct interferometric measurement of the coherence length of an electron wave packet using a Wien filter," Proceedings of the 7th European Congress on Electron Microscopy, 1, 28, 1980.

26. Schmid, H., "Coherence length measurement by producing extremely high phase shifts," Proceedings of the European Congress on Electron Microscopy, 1, 285, 1984.

27. Spence, J.C.H., W. Qian, M.P. Silverman, "Electron source brightness and degeneracy from Fresnel fringes in field emission point projection microscopy," J. Vac. Sci. Techn. A, Vol. 12, 542, 1994.

28. Scheinfein, M.R., W. Qian, J.C.H. Spence, "Aberrations of emission cathodes: nanometer diameter field-emission electron sources," J. Appl. Phys., Vol. 73, 2057, 1993.

29. Briers, J. David, "Laser Doppler and time-varying speckle: a reconciliation," J. Opt. Soc. Am. A, 13, 2, 1996.

30. Lichte, H., G. Möllenstedt, H. Wahl, "A Michelson interferometer using electron waves," Z. Physik, Vol. 249, 456, 1972.

31. Cloud, G., *Optical Methods of Engineering Analysis*, Cambridge University Press, New York, 1995.

32. Haible, P., Kothiyal, M. P., and Tiziani, H. J., "Heterodyne temporal speckle-pattern Interferometry," Applied Optics, 39, 1, 2000.

33. Serway, R. A., *Physics for Scientists and Engineers*, Saunders College Publishing, NY, 1986.

34. Zhou, F., "Coherence and incoherence of inelastically scattered electron waves," Ultramicroscopy, 92, 293, 2002.

35. Spence, J.C.H., J.M. Zou, "Does electron holography energy-filter?" Ultramicroscopy, 69, 185, 1997.

36. Hirayam, T., J. Chen, T. Tanji, A. Tonomura, "Dynamic observation of magnetic domains by on-line real-time electron holography," Ultramicroscopy, 54, 9, 1994.

37. Spence, J.C.H., *High-Resolution Electron Microscopy*, 3rd Edition, Oxford University Press, Oxford, UK, 2003.

38. Brau, C.A., *Free-Electron Lasers*, Academic Press, London, UK, 1990.

39. Shiozawa, T., *Classical Relativistic Electrodynamics*, Springer, Heidelberg, Germany, 2004.

40. Tonomura, A., *Electron Holography*, Springer, Heidelberg, Germany, 1999.

DISTRIBUTION

1	MS0555	Bruce D. Hansche	01522
1	MS0866	Paul Kotula	01822
1	MS0886	Joseph Michael	01822
1	MS1070	Jim Redmond	01526
1	MS1080	Richard Plass	17492
2	MS9018	Central Technical Files	8944
2	MS0899	Technical Library	4536
1	MS0123	D. Chavez, LDRD Office	1011